

Supporting information

Efficient organic solar cells based on a new “Y-series” non-fullerene acceptor with an asymmetric electron-deficient-core

Fangfang Cai^{†a}, Can Zhu^{†a,b}, Jun Yuan^{*a}, Zhe Li^a, , Lei Meng^b, Wei Liu^a, Hongjian Peng^a, Lihui Jiang^a, Yongfang Li^b and Yingping Zou^{*a}

1. General information
2. Fabrication and characterization of organic solar cells
3. Hole mobility and electron mobility measurements
4. Materials
5. Synthesis
6. ¹H NMR and ¹³C NMR
7. Photocurrent versus effective voltage
8. Photocurrent dependence on light intensity.
9. Optical and electrochemical data
10. All detailed photovoltaic data

1. General Information

^1H NMR and ^{13}C NMR spectra were recorded using a Bruker AV-400 spectrometer in a deuterated chloroform solution at 293K. Chemical shift: CHCl_3 ($\delta = 7.26$ ppm for ^1H NMR and $\delta = 77.0$ ppm for ^{13}C NMR). Multiplicities of NMR signal are described as s (signal) or m (multiplet). UV-Vis spectra were measured using a Shimadzu UV-2600 recording spectrophotometer. Cyclic voltammetry (CV) measurements of small molecule acceptor (SMA) thin films were conducted on a CHI660E voltammetric analyzer in tetrabutylammonium hexafluorophosphate (Bu_4NPF_6 , 0.1 M) acetonitrile solutions as conventional three-electrode and using a scan rate of 20 mV s^{-1} . The morphologies of the PM6:Y21 blend films were investigated by atomic force microscopy (AFM, Agilent Technologies, 5500 AFM/SPM System, USA) in contacting mode with a $5 \mu\text{m}$ scanner. Transmission electron microscope (TEM) measurements were performed in a JEM-2100F.

2 Fabrication and characterization of organic solar cells

Reverse device structures were constructed in an ITO/ZnO/active layer/ MoO_3 /Ag configuration. The pre-patterned ITO glass substrates (sheet resistance = $12 \Omega \text{ sq}^{-1}$) were ultrasonicated in detergent, deionized water, acetone, isopropanol and UV-treated in ultraviolet–ozone chamber (Jelight Company, USA) for 20 min. ZnO (Sol-gel) was spin-coated onto the ITO substrate (30 nm) and then the ITO substrates were thermal annealed at $200 \text{ }^\circ\text{C}$ for 1 h in the air. The polymer PM6:Y21 (D:A = 1:1, 16 mg mL^{-1} in total) were dissolved in chloroform (CF) and 1-chloronaphthalene (CN) (0.5 %, v/v) and spin-cast at 3500 rpm for 30s onto the ZnO (Sol-gel) layer (a thickness of $\sim 130 \text{ nm}$). It was then annealed at $100 \text{ }^\circ\text{C}$ for 5 minutes. After cooling to room temperature, the sample is transferred to the evaporation chamber. Under the condition of $1 \times 10^{-5} \text{ Pa}$, 10 nm-thick MoO_3 and about 100 nm of Ag were respectively evaporated. The device area was 5.0 mm^2 .

The conventional device structures were constructed in an ITO/PEDOT:PSS/active layer/PFN-Br/Al configuration. The ITO glass substrates were cleaned as above. PEDOT:PSS film was baked at $150 \text{ }^\circ\text{C}$ for 20 min in the air, and the thickness of the PEDOT:PSS layer was about 30 nm. The preparation methods of the active layer were as described above. Then the bilayer cathode consisting of PFN-Br ($\sim 15 \text{ nm}$) capped with Al ($\sim 120 \text{ nm}$) was thermally evaporated under a shadow mask with a base pressure of ca. 10^{-5} Pa . Finally, top electrodes were deposited in a vacuum onto the active layer. The active area of the device was 5 mm^2 .

The J – V measurement was performed via the solar simulator (SS-F5-3A, Enlitech) along with AM 1.5 G spectra whose intensity was calibrated by the certified standard silicon solar cell (SRC-2020, Enlitech) at 100 mW/cm^2 . The external quantum efficiency (EQE) values were measured by Solar Cell

Spectral Response Measurement System QE-R3-011 (Enli Technology Co., Ltd., Taiwan). The light intensity at each wavelength was calibrated with a standard single-crystal Si photovoltaic cell.

3 Hole mobility and electron mobility measurements

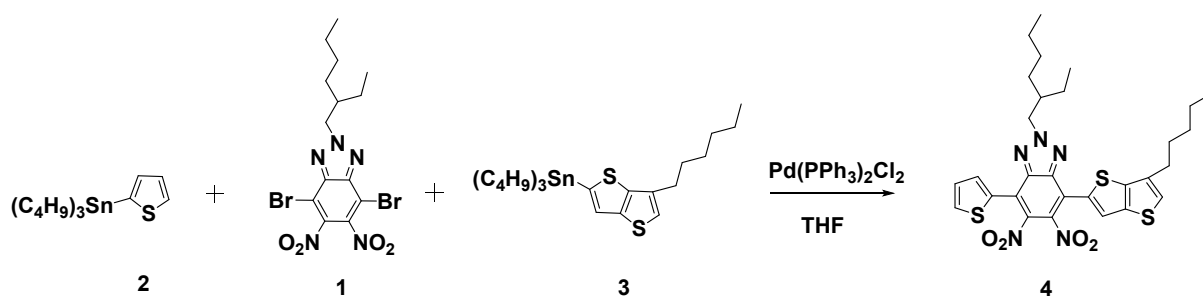
The electron mobility device adopts the ITO/ZnO/active layer/PDINO/Al structure, and the hole mobility device adopts the ITO/PEDOT:PSS/active layer/MoO₃/Ag structure. The hole and electron mobilities are calculated according to the space charge limited current (SCLC) method equation: $J = 9\mu\epsilon_r\epsilon_0V^2/8d^3$, where J is the current density, μ is the hole or electron mobility, V is the internal voltage in the device, ϵ_r is the relative dielectric constant of active layer material, ϵ_0 is the permittivity of empty space, and d is the thickness of the active layer.

4 Materials

Compound 1, compound 2 and compound 3 were synthesized according to the previously reported methods. The PM6, bis(triphenylphosphine)palladium(II) dichloride (Pd(PPh₃)₂Cl₂) and reagents were purchased from business. Tetrahydrofuran (THF) was further dried by using potassium sodium alloy under 110°C refluxing condition. Compound 4 was synthesized by Still-coupling reaction in one-pot method and following that, we can obtain five-membered ring, six-membered ring and seven-membered ring products, respectively.

5 Synthesis

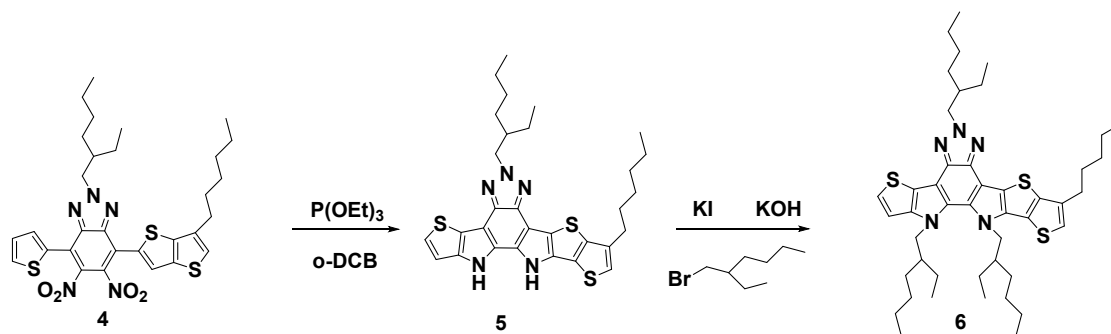
Synthesis of 2-(2-ethylhexyl)-4-(6-hexylthieno[3,2-b]thiophen-2-yl)-5,6-dinitro-7-(thiophen-2-yl)-2H-benzo[d][1,2,3]triazole (compound4):



Compound 2 (2.92g, 7.83mmol), compound 3 (4.02g, 7.83mmol) and compound 1 (2.5g, 5.22mmol) was degassed in dry THF, afterthatPd(PPh₃)₂Cl₂(0.24 g, 0.34 mmol) was added. The mixture was refluxed under argon (Ar) for 24 hours. The reaction mixture was allowed to cool to room temperature and then concentrated under reduced pressure.Crude product was obtained as an orange liquid without further purification. The crude product was chromatographically purified on silica gel column with dichloromethane /hexane (1:8,v/v) as the eluent to afford compound 4 as an orange-yellow solid (2.87 g, 88 %).

$^1\text{H NMR}$ (400 MHz, CDCl_3) δ 7.72 (s, 1H), 7.67 (d, $J = 5.1$ Hz, 1H), 7.55 (d, $J = 3.7$ Hz, 1H), 7.22 – 7.19 (m, 1H), 7.14 (s, 1H), 4.75 (d, $J = 6.8$ Hz, 2H), 2.77 (t, $J = 7.6$ Hz, 2H), 2.29 – 2.20 (m, 1H), 1.77 (t, $J = 11.3$ Hz, 2H), 1.39 – 1.28 (m, 14H), 0.93 (dd, $J = 20.6, 7.2$ Hz, 9H).

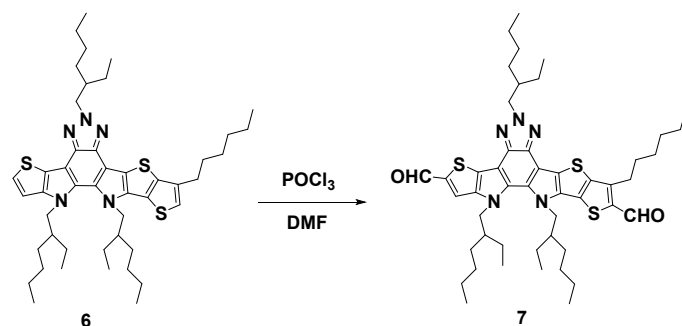
Synthesis of 5,11,12-tris(2-ethylhexyl)-1,8-dihexyl-11,12-dihydro-5H-thieno[2',3':4,5]pyrrolo[3,2-g]thieno[2',3':4,5]thieno[3,2-b][1,2,3]triazolo[4,5-e]indole (compound 6)



Compound 4 (2.87g, 4.58mmol) and triethyl phosphate (50 mL) were dissolved in dichlorobenzene (o-DCB, 20 mL) under nitrogen. The reaction was carried out at 180 °C for 10 hours, extracted with dichloromethane and water, dried, and then evaporated. Crude product (5) was obtained as a dark green liquid without further purification. Crude product 5, 1-bromo-2-ethylhexane (7.9g, 41.22 mmol), potassium iodide (0.34g, 1.8 mmol) and potassium carbonate (2.56 g, 45.8 mmol) were dissolved in the DMF (80 mL). After being heated at 90°C overnight, the reaction was cooled to room temperature. The solution was removed under vacuum and extracted with ethyl acetate and H_2O . The organic layers were combined and dried over MgSO_4 , filtered and purified with column chromatography on silica gel using dichloromethane/petroleum ether (1/8, v/v) as the eluent to give a light-yellow solid (compound 6) (0.76 g, 25% yield).

$^1\text{H NMR}$ (400 MHz, CDCl_3) δ 7.28 (d, $J = 5.1$ Hz, 1H), 7.07 (d, $J = 5.2$ Hz, 1H), 6.88 (s, 1H), 4.64 (d, $J = 7.2$ Hz, 2H), 4.49 (d, $J = 7.6$ Hz, 2H), 4.40 (d, $J = 7.5$ Hz, 2H), 2.73 (t, $J = 7.6$ Hz, 2H), 2.29 (s, 1H), 1.82 (dd, $J = 35.6, 8.2$ Hz, 4H), 1.30 (dd, $J = 18.9, 9.0$ Hz, 14H), 0.90 – 0.70 (m, 25H), 0.56 – 0.44 (m, 12H).

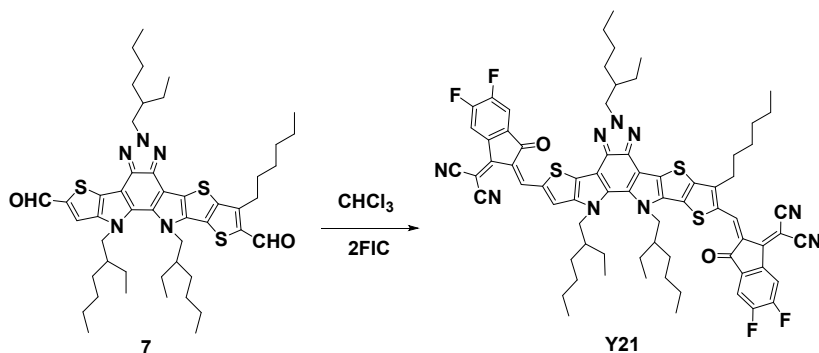
Synthesis of 5,11,12-tris(2-ethylhexyl)-8-hexyl-11,12-dihydro-5H-thieno[2',3':4,5]pyrrolo[3,2-g]thieno[2',3':4,5]thieno[3,2-b][1,2,3]triazolo[4,5-e]indole-2,9-dicarbaldehyde (compound 7)



To a solution of compound 6 (0.76 g, 1.14 mmol) in dry DMF (80 ml) at 0 °C, phosphorus oxychloride (3 ml, 34.35 mmol) was slowly added dropwise under Ar atmosphere. Then stirred additional 2h at 0°C, the solution was heated to 90°C and stirred overnight. The reaction mixture was poured into water (500mL), and then extracted with dichloromethane. After evaporated under reduced pressure, the crude product was purified by column chromatography (petroleum/ dichloromethane) to obtain compound 7 (0.725 g, 75%) as a yellow solid

¹H NMR (400 MHz, CDCl₃) δ 10.14 (s, 1H), 10.01 (s, 1H), 7.84 (s, 1H), 4.73 (d, *J* = 7.1 Hz, 2H), 4.61 (d, *J* = 7.7 Hz, 2H), 4.54 (d, *J* = 7.6 Hz, 2H), 3.20 (t, *J* = 7.7 Hz, 2H), 2.36 (s, 1H), 1.95 – 1.87 (m, 4H), 1.44 – 1.31 (m, 14H), 1.02 – 0.83 (m, 25H), 0.71 – 0.56 (m, 10H), 0.54 (m, 2H).

Synthesis of 2,2'-((2Z,2'Z)-((5,11,12-tris(2-ethylhexyl)-8-hexyl-11,12-dihydro-5H-thieno[2',3':4,5]-pyrrole[3,2-g]thieno[2',3':4,5]thieno[3,2-b][1,2,3]triazolo[4,5-e]indole-2,9-diyl)-bis(methanylylidene))bis(5,6-difluoro-3-oxo-2,3-dihydro-1H-indene-2,1-diylidene))dimalononitrile (Y21)



Compound 7 (0.16 g, 0.19 mmol) and 2-(5,6-difluoro-3-oxo-2,3-dihydro-1H-inden-1-ylidene)-malononitrile (2FIC) (0.2g, 0.76mmol), chloroform (50 mL) were dissolved in a round bottom flask under nitrogen. Then pyridine (1.26 ml) was slowly added dropwise. The solution was heated to 65°C and stirred overnight. After the reaction was completed, the reaction was poured into 200 ml of methanol and the crude product was precipitated. After extraction filtration, the filter residue was extracted with methanol, n-hexane and chloroform for 12 h by using a soxhlet extractor. Finally, the solvent of chloroform-extracted solution was removed the solvent by rotary evaporator, the residue was purified with column chromatography on silica gel using dichloromethane/petroleum ether (3/1, v/v) as the eluent to give a dark blue solid Y21 (0.12 g, 50% yield).

¹H NMR (400 MHz, CDCl₃) δ 9.14 (s, 1H), 9.00 (s, 1H), 8.59 – 8.51 (m, 2H), 8.09 (s, 1H), 7.71 (dd, *J* = 15.9, 7.8 Hz, 2H), 4.72 (t, *J* = 6.5 Hz, 4H), 4.57 (d, *J* = 7.6 Hz, 2H), 3.22 (t, *J* = 7.7 Hz, 2H), 2.38 (s, 1H), 2.00 (d, *J* = 10.7 Hz, 2H), 1.87 (d, *J* = 14.8 Hz, 2H), 1.41 (dd, *J* = 24.4, 16.4 Hz, 14H), 1.09 – 0.81 (m, 25H), 0.71 (t, *J* = 11.2 Hz, 6H), 0.65 – 0.55 (m, 6H).

¹³C NMR (101 MHz, CDCl₃) δ 186.16, 185.82, 158.81, 158.59, 155.71, 153.86, 153.06, 146.93, 145.48, 139.17, 138.79, 136.72, 136.16, 135.71, 135.21, 134.50, 133.44, 132.59, 129.21, 126.76,

121.16 , 119.87 , 114.76 , 113.80 , 112.46 , 110, 68.65 , 59.86 (s), 55.06 , 43.30 – 36.00 , 33.14 – 25.66 ,
26.04 – 19.81 , 16.95 – 12.62 , 12.62 – 8.34 .

6 ^1H NMR and ^{13}C NMR

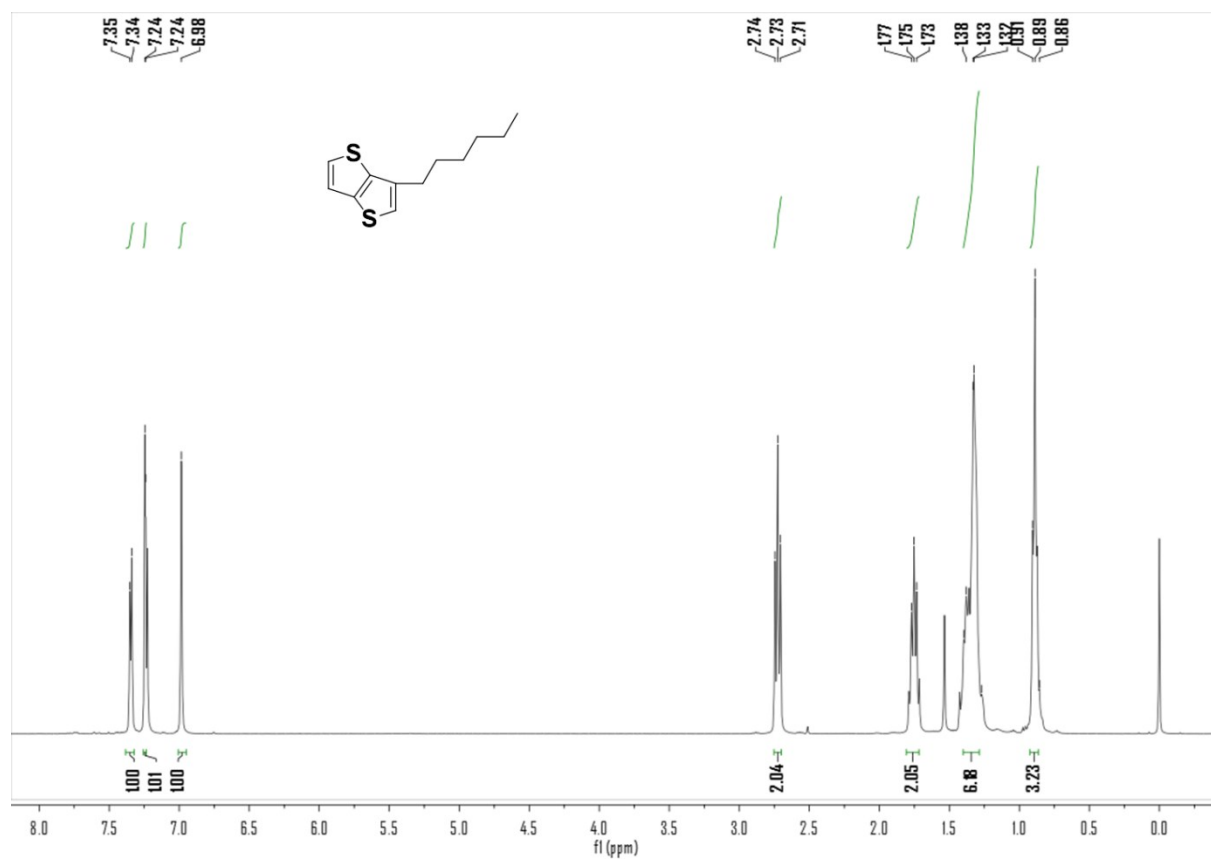


Figure S1. ^1H NMR spectrum of 3-hexylthieno[3,2-b]thiophene.

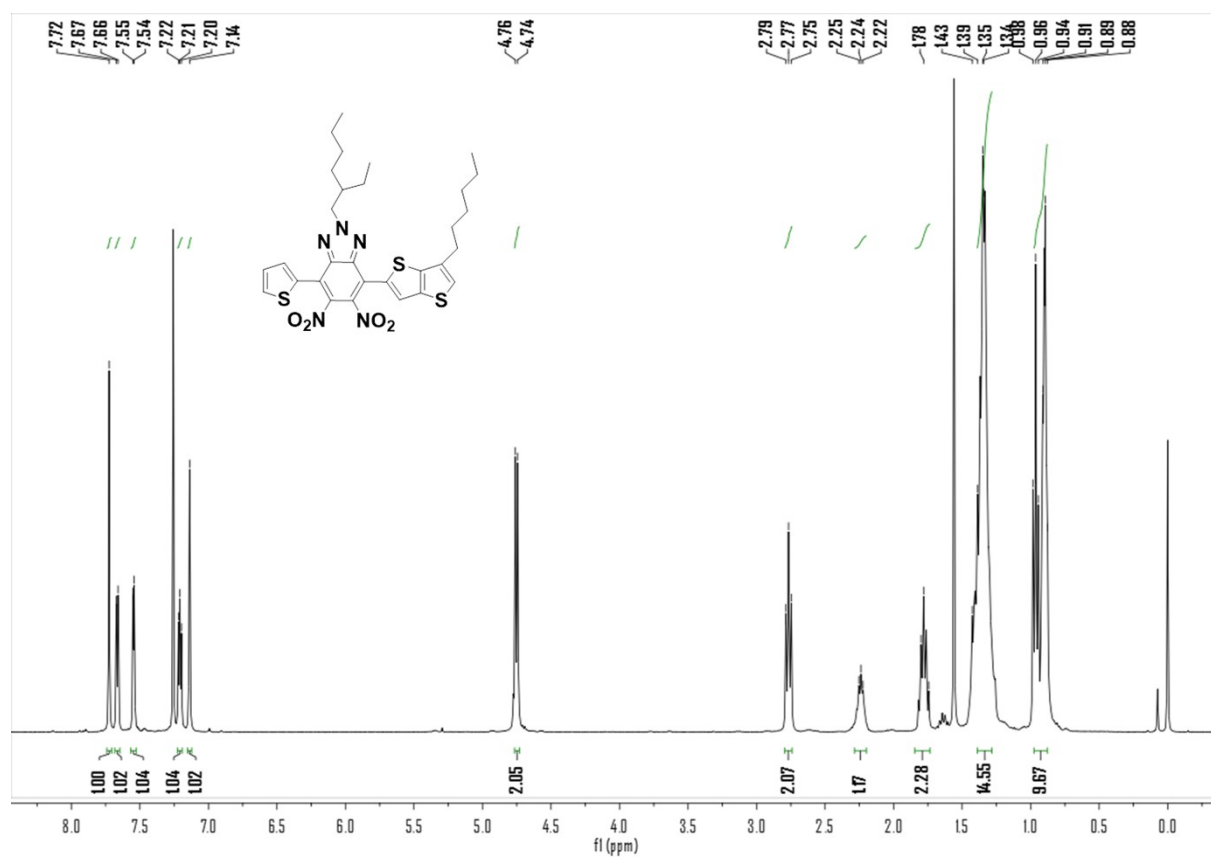


Figure S2. ^1H NMR spectrum of 2-(2-ethylhexyl)-4-(6-hexylthieno[3,2-b]thiophen-2-yl)-5,6-dinitro-7-(thiophen-2-yl)-2H-benzo[d][1,2,3]triazole (compound 4).

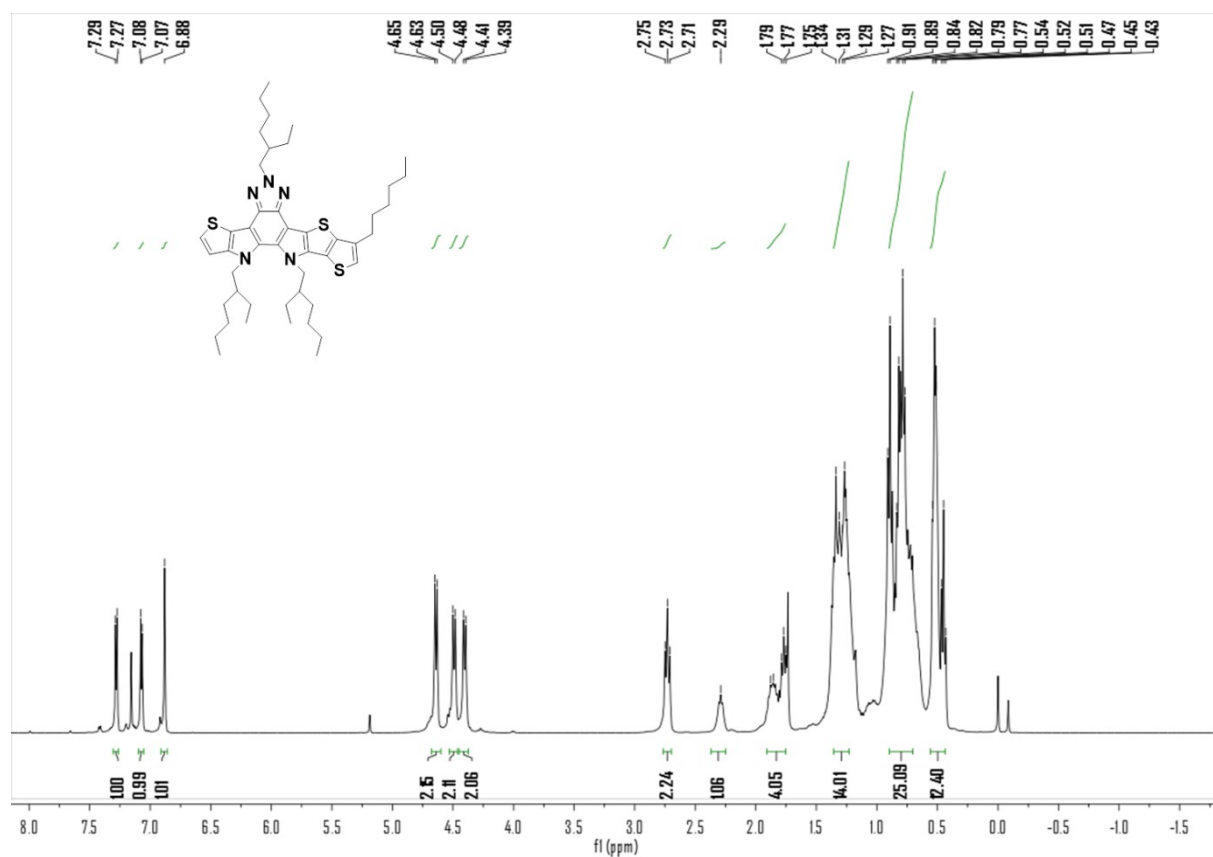


Figure S3. ^1H NMR spectrum of 5,11,12-tris(2-ethylhexyl)-1,8-dihexyl-11,12-dihydro-5H-thieno[2',3':4,5]pyrrolo[3,2-g]thieno[2',3':4,5]thieno[3,2-b][1,2,3]triazolo[4,5-e]indole (compound 6).

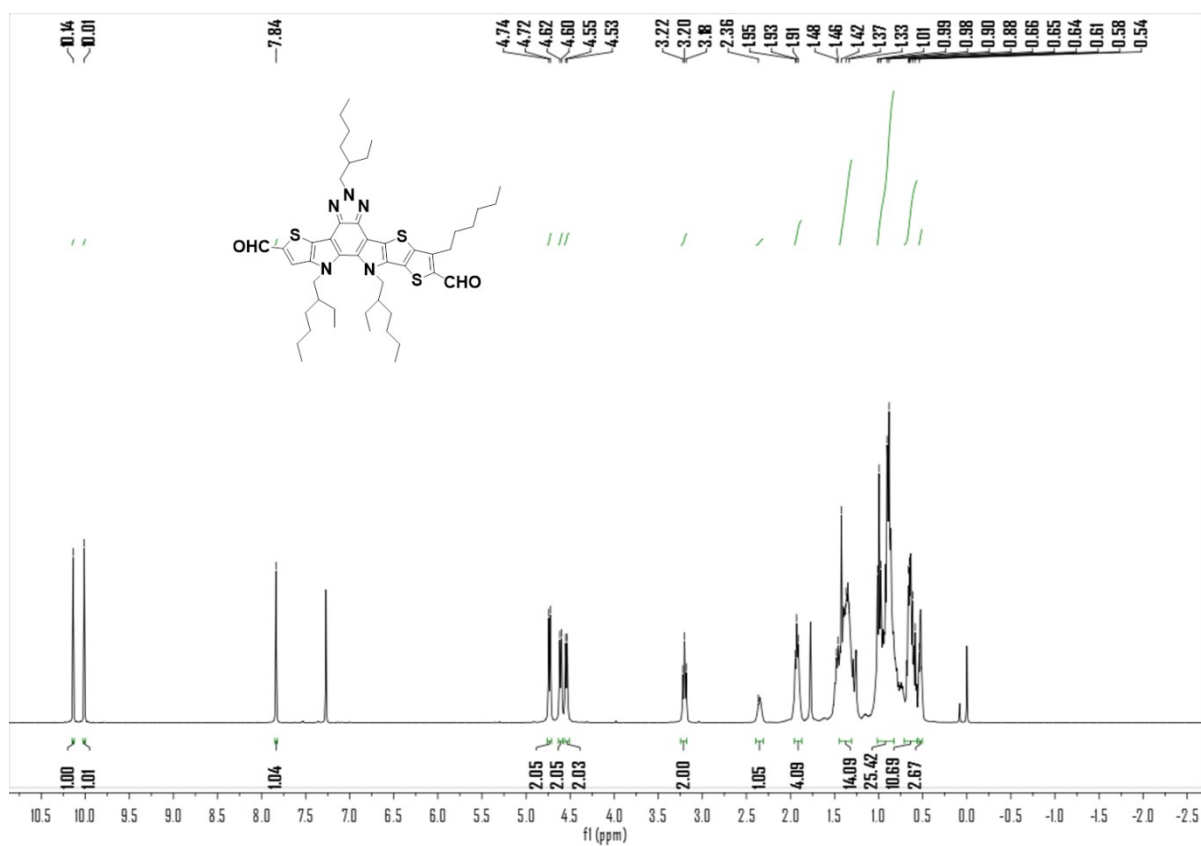


Figure S4. ¹H NMR spectrum of 5,11,12-tris(2-ethylhexyl)-8-hexyl-11,12-dihydro-5H-thieno[2',3':4,5]pyrrolo[3,2-g]thieno[2',3':4,5]thieno[3,2-b][1,2,3]triazolo[4,5-e]indole-2,9-dicarbaldehyde (compound 7).

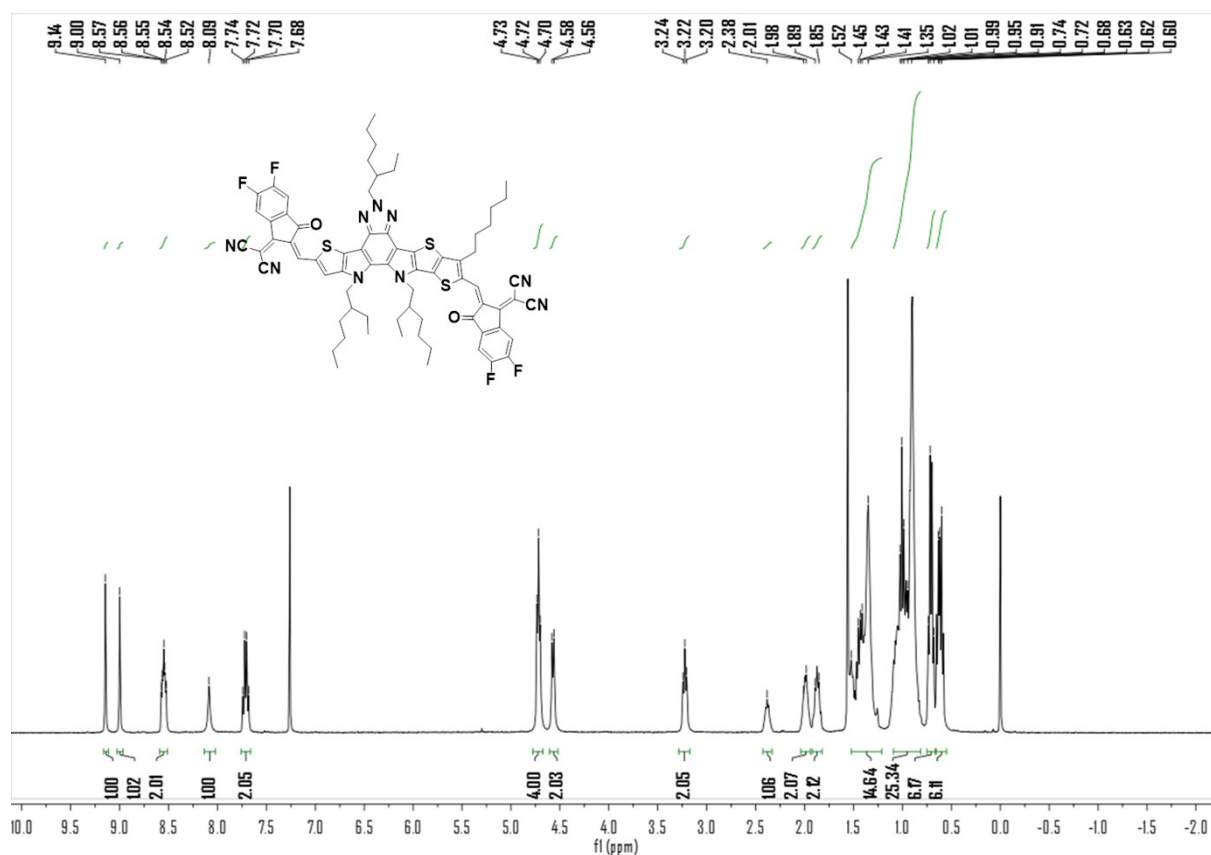


Figure S5. ^1H NMR spectrum of 2,2'-((2Z,2'Z)-((5,11,12-tris(2-ethylhexyl)-8-hexyl-11,12-dihydro-5H-thieno[2',3':4,5]-pyrrole[3,2-g]thieno[2',3':4,5]thieno[3,2-b][1,2,3]triazolo[4,5-e]indole-2,9-diyl)-bis-(methanylylide-ne))bis(5,6-difluoro-3-oxo-2,3-dihydro-1H-indene-2,1-diylidene))dimalononitrile (Y21).

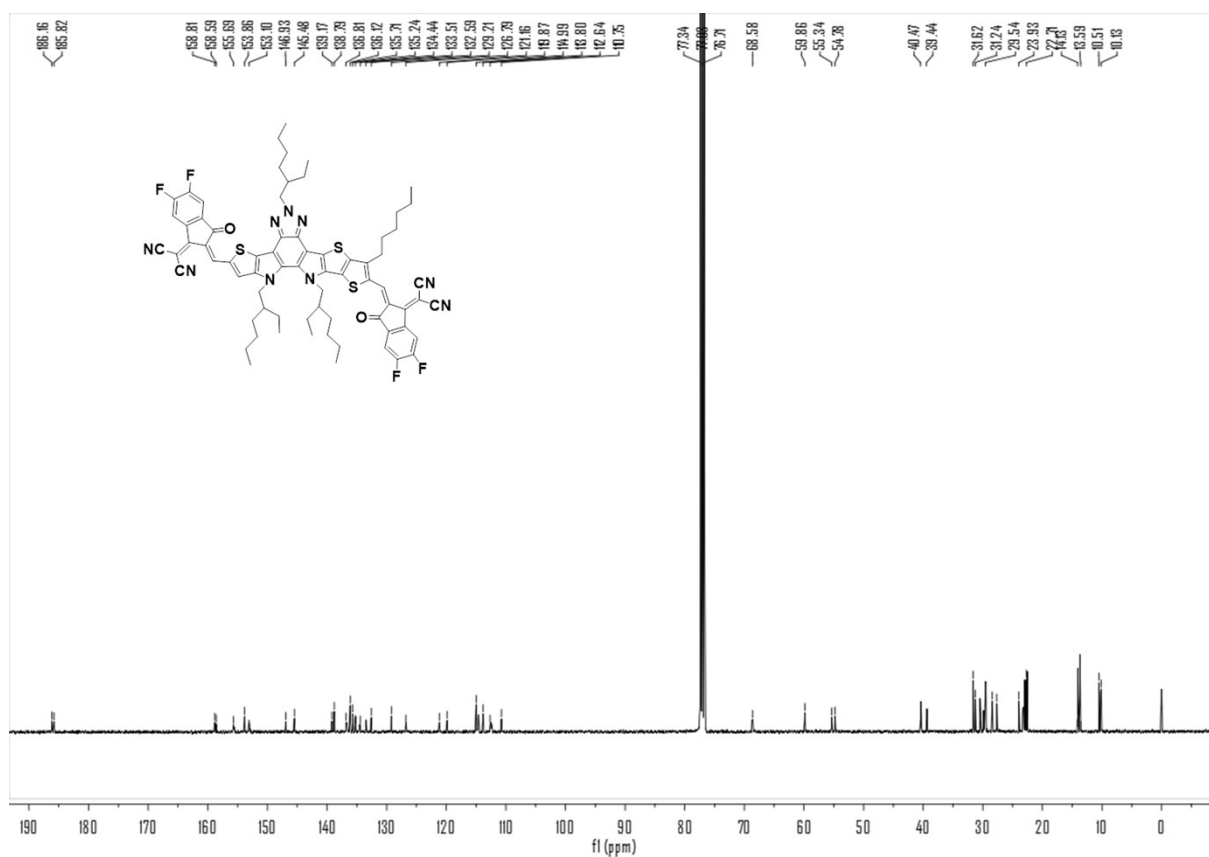


Figure S6. ^{13}C NMR spectrum of 2,2'-((2Z,2'Z)-((5,11,12-tris(2-ethylhexyl)-8-hexyl-11,12-dihydro-5H-thieno[2',3':4,5]-pyrrole[3,2-g]thieno[2',3':4,5]thieno[3,2-b][1,2,3]triazolo[4,5-e]indole-2,9-diyl)-bis-(methanylylide-ne))bis(5,6-difluoro-3-oxo-2,3-dihydro-1H-indene-2,1-diylidene))dimalononitrile (Y21).

7 Photocurrent versus effective voltage

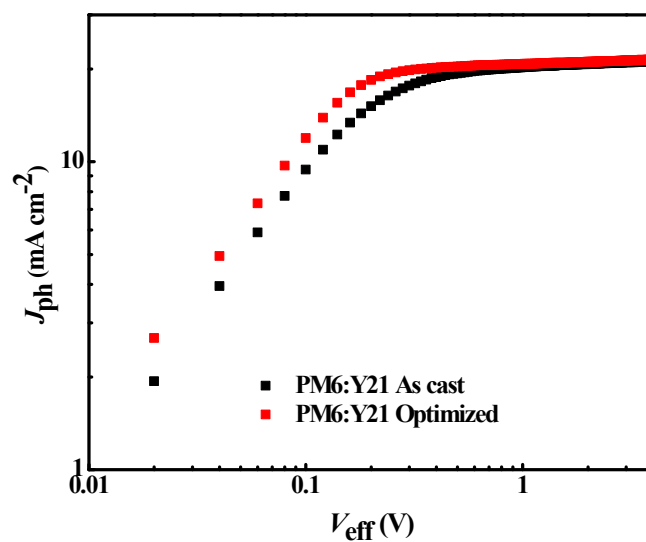


Figure S7. Photocurrent versus effective voltage of the as-cast and optimized devices based on PM6:Y21 (1:1, w/w) blend.

8 Photocurrent dependence on light intensity.

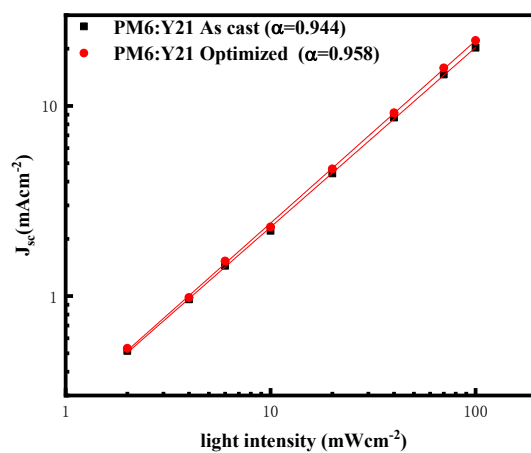


Figure S8. Photocurrent versus light intensity of the as-cast and optimized devices based on PM6:Y21.

9 Optical and electrochemical data

Table S1: Optical and electrochemical properties of Y21

	Absorption spectra				Cyclic voltammetry		
	Sol ^a		Film ^b		<i>p</i> -doping	<i>n</i> -doping	
	λ_{\max} (nm)	λ_{\max} (nm)	λ_{onset} (nm)	E_g^{opt} ^c (eV)	$E_{\text{on}}^{\text{ox}}$ /HOMO (V)/(eV)	$E_{\text{on}}^{\text{red}}$ /LUMO (V)/(eV)	E_g^{EC} (eV)
Y21	741	826	917	1.35	1.28/-5.64	-0.33/-4.03	1.6
PM6	550	614	684	1.81	1.20/-5.56	-0.86/-3.50	2.0
Y6	731	821	931	1.33	1.29/-5.65	-0.26/-4.10	1.5

a. Measured in chloroform solution. b. Cast from chloroform solution. c. Bandgap estimated from the onset wavelength of the optical absorption.

10 All detailed photovoltaic data

Table S2. Optimization of the inverted devices with D/A ratio, additive and annealing temperature for Y21-based blend films under illumination of AM 1.5G, 100 mW cm⁻²

Ratio	concentration	Additive (%)	Annealing (°C)	V _{oc} (V)	J _{sc} (mA/cm ²)	FF (%)	PCE (%)
1:1	16 mg/ mL	/	/	0.845	24.30	67.19	13.79
		CN(0.5)	100	0.833	24.87	74.43	15.42
1:1.2		/	/	0.821	22.55	62.5	11.57
		CN(0.5)	110	0.813	22.60	73.05	13.42
			/	/	0.86	21.55	71.82
1.5		CN(0.5)	110	0.815	22.89	74.21	13.84

Table S3. Optimization of the conventional devices with D/A ratio, additive and annealing temperature for Y21-based blend films under illumination of AM 1.5G, 100 mW cm⁻²

Ratio	concentration	Additive (%)	Annealing (°C)	V _{oc} (V)	J _{sc} (mA/cm ²)	FF (%)	PCE (%)
1:1	16 mg/ mL	CN(0.5)	100	0.840	23.54	70.2	13.88

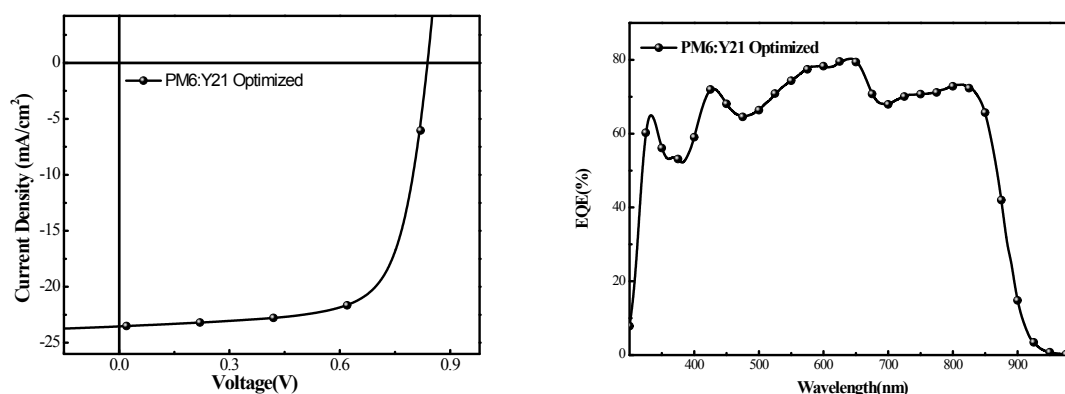


Figure S9. Current density versus voltage characteristic and EQE curve of the conventional device